Published in final edited form as:
Hepatology. 2014 April ; 59(4): 1577–1590. doi:10.1002/hep.26898.

EGFR inhibition attenuates liver fibrosis and development of hepatocellular carcinoma

Bryan C. Fuchs[1], **Yujin Hoshida**[2], **Tsutomu Fujii**[1], **Lan Wei**[1], **Suguru Yamada**[1], **Gregory Y. Lauwers**[3], **Christopher M. McGinn**[4], **Danielle K. DePeralta**[1], **Xintong Chen**[2], **Toshihiko Kuroda**[1], **Michael Lanuti**[4], **Anthony D. Schmitt**[4], **Supriya Gupta**[5], **Andrew Crenshaw**[5], **Robert Onofrio**[5], **Bradley Taylor**[5], **Wendy Winckler**[5], **Nabeel Bardeesy**[6], **Peter Caravan**[7], **Todd R. Golub**[8,9,10], and **Kenneth K. Tanabe**[1]

[1]Division of Surgical Oncology, Massachusetts General Hospital Cancer Center and Harvard Medical School, 55 Fruit Street, Boston, MA, 02114

[2]Liver Cancer Program, Tisch Cancer Institute, Division of Liver Diseases, Department of Medicine, Icahn School of Medicine at Mount Sinai

[3]Department of Pathology, Massachusetts General Hospital Cancer Center and Harvard Medical School, 55 Fruit Street, Boston, MA, 02114

[4]Division of Thoracic Surgery, Massachusetts General Hospital Cancer Center and Harvard Medical School, 55 Fruit Street, Boston, MA, 02114

[5]Genetic Analysis Platform, Broad Institute, 7 Cambridge Center, Cambridge MA, 02142

[6]Department of Medicine, Massachusetts General Hospital Cancer Center and Harvard Medical School, 185 Cambridge Street, Boston, MA, 02114

[7]A.A. Martinos Center for Biomedical Imaging, Department of Radiology, Massachusetts General Hospital and Harvard Medical School, 149 Thirteenth St., Suite 2301, Charlestown MA 02129

[8]Cancer Program, Broad Institute, 7 Cambridge Center, Cambridge, MA, 02142

[9]Dana-Farber Cancer Institute and Harvard Medical School, 450 Brookline Avenue, Boston, MA, 02215

[10]Howard Hughes Medical Institute, 20 Shattuck Street, Boston, MA, 02115

Abstract

Hepatocellular carcinoma (HCC) is the most rapidly increasing cause of cancer-related mortality in the United States. Because of the lack of viable treatment options for HCC, prevention in high risk patients has been proposed as an alternative strategy. The main risk factor for HCC is cirrhosis and several lines of evidence implicate epidermal growth factor (EGF) in the progression of cirrhosis and development of HCC. We therefore examined the effects of the EGF receptor (EGFR) inhibitor erlotinib on liver fibrogenesis and hepatocellular transformation in three

Corresponding authors: Kenneth K. Tanabe, Massachusetts General Hospital, Yawkey 7.924, 55 Fruit Street, Boston, MA 02114, (p) 617-724-3868, (f) 617-724-3895, ktanabe@partners.org.
Yujin Hoshida and Tsutomu Fujii contributed equally to this work.

different animal models of progressive cirrhosis – a rat model induced by repeated, low dose injections of diethylnitrosamine (DEN), a mouse model induced by carbon tetrachloride (CCl_4) and a rat model induced by bile duct ligation (BDL). Erlotinib reduced EGFR phosphorylation in hepatic stellate cells (HSC), and reduced the total number of activated HSC. Erlotinib also decreased hepatocyte proliferation and liver injury. Consistent with all these findings, pharmacological inhibition of EGFR signaling effectively prevented the progression of cirrhosis and regressed fibrosis in some animals. Moreover, by alleviating the underlying liver disease, erlotinib blocked the development of HCC and its therapeutic efficacy could be monitored with a previously reported gene expression signature predictive of HCC risk in human cirrhosis patients.

Conclusion—These data suggest that EGFR inhibition with FDA-approved inhibitors presents a promising therapeutic approach for reduction of fibrogenesis and prevention of HCC in high risk cirrhosis patients who can be identified and monitored by gene expression signatures.

Keywords

erlotinib; cirrhosis; prevention; gene expression signatures; CCl_4

Introductory Statement

Hepatocellular carcinoma (HCC) is the sixth most common cancer worldwide, and due to its poor prognosis it is the third leading cause of cancer-related death [1]. In the United States, HCC is the most rapidly increasing cause of cancer-related mortality [2]. While the cause of HCC is multifactorial, the common pathway for the vast majority of cases is cirrhosis. Cirrhosis is estimated to affect 1-2% of the world's population [3]. Nearly one million people die from cirrhosis worldwide each year, and the annual cost for caring for complications of cirrhosis in the United States alone is estimated to be $4 billion. The major clinical consequences of cirrhosis are impaired liver function, portal hypertension, impaired cognitive function and development of HCC, all of which increase the risk of death. Given the lack of successful treatment options for HCC, new strategies for the prevention of HCC by slowing the natural history of liver fibrosis and cirrhosis are urgently needed [4].

Epidermal growth factor (EGF) plays a role in both cirrhosis and HCC. EGF expression in the liver increases during cirrhosis [5]. EGF is also a key member of a 186-gene signature predictive of progressive cirrhosis, HCC development, and death in patients with cirrhosis [6, 7]. In addition, a polymorphism in the human *EGF* gene that leads to increased EGF expression is associated with increased fibrosis and cirrhosis progression [8, 9] and elevated risk of developing HCC in patients with cirrhosis [10]. Finally, transgenic mice with liver-specific overexpression of EGF rapidly develop HCC [11].

We report here that the small-molecule EGF receptor (EGFR) inhibitor erlotinib inhibits the activation of myofibroblastic hepatic stellate cells (HSC), prevents the progression of cirrhosis, regresses fibrosis in some animals and blocks subsequent development of HCC in rodent models.

Experimental Procedures

For details please see Supplementary Information.

Animal Models

Animals received humane care according to the criteria outlined in the "Guide for the Care and Use of Laboratory Animals" of the National Academy of Sciences. All animals were maintained in accordance with the guidelines of the Massachusetts General Hospital Subcommittee on Research Animal Care. Animals were treated as described in the Supplementary Information.

Primary rat HSC isolation

HSC were isolated and cultured as described in the Supplementary Information.

Histology, immunohistochemistry, immunofluorescence and hydroxyproline analysis

Formalin-fixed samples were embedded in paraffin, cut into 5 μm-thick sections, stained and analyzed as described in the Supplementary Information.

Liver Function Tests

A cardiac terminal blood withdrawal was performed at the time of sacrifice and serum was isolated and analyzed as described in the Supplementary Information.

Hydroxyproline analysis and western blotting

Hydroxyproline analysis and western blot analysis are described in the Supplementary Information.

Microarray Analysis

Genome-wide gene expression profiling for the rats and mice was performed using RatRef-12 and Mouse Ref-8 Expression BeadChip microarrays, respectively (Illumina, San Diego, CA) as described in the Supplementary Information.

Statistical Analysis

An unpaired two-tailed t-test was used to compare differences in body weights, liver weights, liver function tests, number of tumors, hydroxyproline levels, western blot densitometry and quantifications of Sirius-red and Ki67 stainings. Differences in Ishak scores were assessed by a Kruskall-Wallis test followed by post hoc Dunn-Holland-Wolfe in the diethylnitrosamine (DEN) and carbon tetrachloride (CCl_4) studies and by a Mann Whitney test in the bile duct ligation (BDL) study. Fisher's exact test was used to assess differences in tumor size.

Results

Erlotinib inhibits DEN-induced rat liver fibrosis

In order to test the hypothesis that EGFR blockade would ameliorate cirrhosis progression and prevent HCC, we evaluated the EGFR tyrosine kinase inhibitor erlotinib in animal models of chronic liver disease. Repeated injections of low-dose DEN (50 mg/kg weekly) in rats causes progressive liver fibrosis and cirrhosis followed by HCC [12, 13]. We used the scoring scale for fibrosis/cirrhosis described by Ishak [14] that ranges from 1 (minimal fibrosis) to 6 (cirrhosis) (Supplementary Table 1). DEN injury for 8 weeks caused fibrosis, with a median Ishak score of 1.0 (interquartile range (IQR) 0.25–1.0; Supplementary Figure 1). After 12 weeks of DEN injury the animals exhibited advanced fibrosis, and many also had cirrhosis, with a median Ishak score of 4.0 (IQR 3.0–5.0; Supplementary Figure 1). By 18 weeks of DEN injury, all animals had marked liver fibrosis and cirrhosis, with a median Ishak score of 5.0 (IQR 4.0–6.0; Supplementary Figure 1). We also morphometrically analyzed disease by quantifying collagen in Sirius red stained sections and observed a progressive increase in staining which was consistent with the Ishak scores (Supplementary Figure 1).

We treated DEN-injured rats with erlotinib at the first signs of cirrhosis (week 13) via an intraperitoneal (IP) injection of either 0.5 or 2 mg/kg (N=8 for each dose), 5 days/week for a total of 6 weeks and compared to vehicle-treated controls (N=16). As noted above, DEN injury alone resulted in macroscopically evident liver fibrosis and nodular cirrhosis. In contrast, livers from DEN animals treated with erlotinib had less severe cirrhosis (Figure 1A). Further, histologic examination of liver sections stained by Masson's trichrome revealed less severe fibrosis and cirrhosis in erlotinib-treated rats, and a doseresponse relationship was observed (Figure 1B). Rats receiving 2 mg/kg erlotinib had median week 18 Ishak scores of 2.0 (IQR 2.0–4.0) that were significantly improved compared to vehicle-treated animals (median Ishak score 5.5, IQR 4.0–6.0; $p < 0.01$; Figure 1C). Animals receiving the 0.5 mg/kg dose had an intermediate improvement (median Ishak score 4.0, IQR 4.0–4.8). Consistent with the Ishak scores, erlotinib was shown to significantly reduce collagen levels dose-dependently in both Sirius red stained sections ($p < 0.01$; Figure 1D) and by hydroxyproline analysis ($p < 0.05$; Figure 1E).

Liver function tests to assess injury and synthetic function demonstrated comparable results between rats injured with DEN and what is observed in humans (Supplementary Figure 2). Treatment with erlotinib slightly improved several biochemical markers of liver injury and cholestasis including serum alkaline phosphatase (ALP), alanine transaminase (ALT), aspartate transaminase (AST) and total bilirubin (TBIL) (Figure 1F). Erlotinib also restored some synthetic function as assessed by significant ($p < 0.01$) increases in serum glucose (Glu) levels but no changes were seen in serum albumin (Alb) levels.

To examine whether erlotinib may regress fibrosis and cirrhosis in some animals, we repeated the study and performed liver wedge biopsies before DEN-injured rats received 2 mg/kg erlotinib (N=8) or vehicle (N=8), and then again after 6 weeks of treatment. This experimental design allows for the measurement of disease progression over time within the same animal. Recognizing that underlying disease might progress differently in this

experimental design which adds in an element of regeneration, we did observe that Ishak scores significantly increased between 12 and 18 weeks in rats that received vehicle but not erlotinib ($p < 0.01$; Figure 2). Importantly, we also observed that erlotinib reversed histological fibrosis in 2 out of 8 animals, and all of these results were confirmed by morphometrically quantifying collagen in Sirius red stained sections ($p < 0.01$; Figure 2).

Erlotinib inhibits CCl_4-induced mouse liver fibrosis

We also tested the effects of erlotinib on fibrogenesis in the well-characterized CCl_4 mouse model. Mice injured with CCl_4 by oral gavage reliably develop liver fibrosis after 18 weeks [15]. Treatment with erlotinib (either 2 or 5 mg/kg) beginning at 13 weeks inhibited fibrogenesis as indicated by Sirius red staining (Figure 3A). Trichrome stains were scored and mice receiving 2 mg/kg erlotinib had median week 18 Ishak scores of 1.0 (IQR 0.0–2.5), while mice receiving 5 mg/kg erlotinib had median week 18 Ishak scores of 1.0 (IQR 0.0–2.0). Both groups were significantly improved compared to vehicle-treated controls (median week 18 Ishak score 3.0, IQR 2.3–3.8; $p < 0.05$; Figure 3B). Erlotinib was further shown to reduce collagen levels in Sirius red stained sections ($p < 0.01$; Figure 3C) and also by hydroxyproline analysis (Figure 3D) but the latter results did not reach significance. Interestingly, erlotinib had a much greater effect of reducing liver injury in this model as assessed by decreases in serum ALT and AST levels and again increased serum Glu levels (Figure 3E).

Both DEN-injured rats and CCl_4-injured mice represent models of parenchymal liver fibrosis [16]. DEN and CCl_4 are primarily metabolized and activated by cytochrome P450 2E1 (CYP2E1) [17, 18] and thus erlotinib could inhibit disease progression in these models by inhibiting the expression of CYP2E1. However, we observed that whereas DEN and CCl_4 injury alone significantly decreased the expression of CYP2E1, treatment with erlotinib slightly increased its expression (Supplementary Figure 3) as well as the expression of several other CYPs and drug metabolizing enzymes (Supplementary Table 2).

Erlotinib inhibits BDL-induced rat liver fibrosis

Next, we examined the effects of erlotinib on biliary fibrosis induced by BDL in rats. BDL caused liver fibrosis that progressed to liver cirrhosis within a few weeks. Treatment with 2 mg/kg erlotinib beginning at 4 days after the BDL inhibited fibrogenesis as indicated by Sirius red staining (Figure 4A). In addition, BDL caused a significant increase in liver weight which was partly attenuated by erlotinib ($p < 0.01$; Figure 4B). Trichrome stains were scored and rats receiving 2 mg/kg erlotinib had median day 21 Ishak scores of 4.0 (IQR 3.0–4.0), which were significantly improved compared to vehicle-treated controls (median day 21 Ishak score 5.0, IQR 4.0–6.0; $p < 0.01$; Figure 4C). Consistent with the Ishak scores, erlotinib was shown to reduce collagen levels in both Sirius red stained sections ($p < 0.01$; Figure 4D) and by hydroxyproline analysis ($p < 0.05$; Figure 4E). Similar to the DEN model, erlotinib only had slight effects on liver injury after BDL but again significantly ($p < 0.01$) increased serum Glu levels (Figure 4F).

Erlotinib reverses a human cirrhosis poor-prognosis gene signature

Interestingly, while a recent study has demonstrated that rodent models in response to a variety of stimuli poorly mimic genomic immunological responses in humans [19], we found that deregulation of liver fibrosis/cirrhosis-related molecular pathways in several rodent models of chronic liver disease did resemble human cirrhosis (Supplementary Figure 4). The DEN rat model constantly showed a more similar pattern to human cirrhosis compared to these other models.

We also evaluated the DEN rat model of cirrhosis using a previously reported 186-gene expression signature predictive of liver cirrhosis progression and risk of HCC [6, 7]. This signature consists of 73 poor-prognosis-correlated genes and 113 good-prognosis-orrelated genes expressed in cirrhotic liver tissue (Supplementary Table 3). We observed that the poor-prognosis genes were already significantly induced by 8 weeks of DEN injury, and the good-prognosis genes were down-regulated over time (Supplementary Figure 5). When compared to the other rodent models of chronic liver disease, the DEN rat model better reproduces this human cirrhosis gene signature as well (Supplementary Table 4).

In response to erlotinib, expression of the poor-prognosis genes decreased, while expression of the good-prognosis genes increased, both in a dose-dependent fashion (false discovery rate (FDR)=0.002 and < 0.001, respectively; Figure 5A-B). Similar effects of erlotinib were observed in CCl_4-injured mice (Supplementary Figure 6). We also observed that erlotinib inhibited the expression of several known pro-fibrogenic genes that were up-regulated in response to DEN (Figure 5C). These results correlate well with the gross and histopathological observations demonstrating inhibition of cirrhosis in response to erlotinib. In addition, the 186-gene signature may serve as a useful biomarker of erlotinib response.

Erlotinib inhibits EGFR signaling in DEN-treated rats

EGF expression normally increases over time in DEN-injured rats [20], and we observed an increase in several other EGFR ligands as well (Supplementary Figure 7). Consistently, we observed an increase in the ratio of phospho-EGFR/total EGFR and a decrease in total EGFR levels in non-tumor bearing liver (Figure 6A,B). These findings are consistent with ligand-mediated receptor endocytosis that occurs following activation of the pathway [21]. The level of p44/42 mitogen-activated protein kinase (ERK) activation in the livers from DEN-injured rats correlated with proliferation as assessed by proliferating cell nuclear antigen (PCNA) expression (Figure 6A,B). DEN-induced EGF pathway activation is also evidenced by two separate and independently defined gene-expression signatures of experimental EGF pathway activation (Supplementary Figure 8). These data provide multiple lines of evidence of EGFR activation in DEN-injured rat cirrhosis, similar to that observed in human cirrhosis.

To establish that EGFR, the principal target of erlotinib, was inhibited in treated animals, we performed western blot analysis to examine EGFR signaling in DEN-injured livers. Erlotinib significantly inhibited EGFR activation in the non-tumoral liver tissue as indicated by decreased levels of phospho-EGFR as well as increased levels of total EGFR - a known feedback response to EGFR inhibition (Figure 6C,D). EGF pathway activation signatures

that were enriched in DEN-injured livers were also significantly down-regulated in response to erlotinib (Supplementary Figure 8). Further, erlotinib decreased ERK activation and PCNA in the non-tumoral tissue (Figure 6C,D).

EGFR expression varies between the different cell populations in the liver with high expression observed in hepatocytes and HSC but relatively little expression in Kupffer cells [22]. EGFR is known to be an important regulator of hepatocyte regeneration [23], and upon treatment with erlotinib, we noticed decreased phospho-EGFR in regenerating nodules (Figure 6E). Interestingly, we also observed decreased phospho-EGFR staining in cells located within the fibrotic bands, which might represent HSC. Consistently, Ki67 staining showed decreased proliferation of these same two cell populations (Figure 6E,F).

Erlotinib treatment is associated with decreased HSC activation

In all three animal models, erlotinib reduced liver injury which is one potential mechanism by which fibrosis progression is inhibited. We also investigated the effects of erlotinib on EGFR activation in HSC. Myofibroblastic HSC play a critical role in promoting liver fibrogenesis [24] and express platelet-derived growth factor receptor-beta (PDGFR-β) and alpha-smooth muscle actin (α-SMA) [25] which thus serve as markers of the activated state. We observed that DEN injury increased HSC activation over time as assessed by α-SMA staining (Figure 7A), and that the sites of α-SMA staining localized to sites of collagen deposition, consistent with the causal role of HSC in liver fibrosis.

EGF is a known soluble mediator involved in HSC activation [25], and HSC are activated by EGFR signaling [26, 27]. We assessed the phosphorylation of EGFR in activated HSC through dual immunofluorescence staining with several well-established HSC markers including α-SMA, desmin and glial fibrillary acidic protein (GFAP). While very little expression of phospho-EGFR was observed in PBS control livers (Figure 7B), the levels increased in the DEN-injured livers and co-localized with HSC markers in cells surrounding the portal tracts and within the collagen bands (Figure 7B). This colocalization was similar to that observed in human cirrhotic livers (Supplementary Figure 9).

Erlotinib significantly decreased the activation of HSC in a dose-dependent fashion in DEN-injured rats, CCl_4-injured mice and BDL rats as assessed by α-SMA expression (Figure 7C; Supplementary Figure 6 and Supplementary Figure 10). In liver sections from DEN-injured rats that received 2 mg/kg erlotinib, phospho-EGFR staining was mostly absent, and even though residual staining of HSC markers was observed, these markers no longer co-localized with the very low levels of phospho-EGFR (Figure 7B).

Data from *in vitro* experiments with HSC reveal similar findings. EGFR expression was observed in isolated, enriched populations of primary rat HSC only after they had been activated in culture as assessed by the expression of PDGFR-β and α-SMA (Figure 7D). In addition, treatment of these activated primary HSC with EGF increases phospho-EGFR, decreases total EGFR and increases phospho-ERK consistent with the DEN rat tissue western blots (Figure 7E). Similar results were also seen after EGF treatment of the human HSC cell line TWNT-4 (Supplementary Figure 9). Importantly, erlotinib significantly suppressed the expression of α-SMA and α1(I) procollagen in TWNT-4 cells

(Supplementary Figure 9) consistent with a role of EGFR inhibition in reducing HSC activation.

Erlotinib inhibits HCC development

We observed that DEN injury caused a loss of total body weight with an elevated ratio of liver weight to body weight as a consequence of the development of well-differentiated HCCs (17 HCCs on average per animal compared to 0 in controls; $p < 0.001$; Supplementary Figure 1). HCCs were observed only in cirrhotic livers as is most commonly seen in humans.

A predicted consequence of the anti-cirrhotic effect of EGFR inhibition is that erlotinib treatment would also abrogate HCC development in cirrhosis. As predicted, erlotinib treatment significantly decreased the number of HCC tumors detectable after 18 weeks of DEN injury. Control animals harbored 20.4±5.5 tumors, whereas erlotinib at 2 mg/kg and 0.5 mg/kg harbored only 5.0±2.2 (75% reduction) and 10.4±3.8 tumors (49% reduction), respectively ($p < 0.01$ for each dose; Figure 8A). Consistent with this finding, liver weights of rats treated with 2 mg/kg erlotinib were reduced by 24% ($p < 0.05$), while liver weights of rats treated with 0.5 mg/kg erlotinib were reduced by 15% ($p=0.15$) (Fig. 8B).

Whereas EGFR inhibition in the non-tumoral liver tissue was clearly observed (Figure 4D, Supplementary Figure 8), no effect of erlotinib on EGFR signaling was seen within HCCs themselves (Figure 8C,D), and no effect of erlotinib on the EGF pathway activation gene signatures was seen in RNA isolated from tumors (Supplementary Figure 8). In addition, tumors that developed in both DEN-injured and erlotinib-treated animals were pathologically similar (Figure 8E), and there were no significant differences in global gene expression (data not shown). In addition, no differences were observed in Ki67 staining of tumors from rats treated with erlotinib or vehicle (Figure 8E). Further, while the number of large tumors (defined as > 8 mm diameter, the 75^{th} percentile) was similar in DEN-injured and erlotinib-treated animals, the number of smaller tumors was dramatically decreased in the erlotinib animals (Figure 8F). These results suggest that erlotinib inhibits initiation of new liver neoplasms rather than suppresses growth of the lesions already present by the time erlotinib was started.

Discussion

The results of our investigation tie together several important observations. The first is that gene expression analyses have demonstrated that the EGF pathway is associated with progression of cirrhosis to mortality [6, 7]. Likewise, in cirrhotic patients, the level of EGF mRNA expression in the cirrhotic tissues is associated with poor survival, whereas tumoral EGF expression in these same patients is not associated with survival (Supplementary Figure 11). Second, HSC play a pivotal role in hepatic fibrogenesis, and EGFR signaling has been shown to activate these cells [26, 27]. Third, polymorphism studies [10] and transgenic mouse models [11] have implicated EGF in hepatocellular transformation to HCC. Nonetheless, a common pathway to HCC is via progressive cirrhosis, and thus, effective strategies that limit or even regress hepatic fibrogenesis are expected to reduce the frequency of HCC.

Given the strong evidence implicating EGF and EGFR in these processes, there is strong rationale to test an EGFR inhibitor for its ability to inhibit hepatic fibrogenesis and hepatocellular transformation. We observed that the FDA-approved EGFR inhibitor erlotinib, used at doses equivalent to or less than those used in humans, significantly reduced fibrogenesis in three separate animal models. Our results suggest that these models are similar with respect to fibrosis resolution but clearly differences do exist with respect to liver injury. Liver injury is more severe in the CCl_4 model and this may be attributable to species differences, the different chemicals themselves or the three times per week dosing with CCl_4 as opposed to once a week dosing with DEN. To examine this further, we used gene set enrichment analysis (GSEA) to evaluate in the DEN-injured rats and CCl_4-injured mice the effect of erlotinib on genes associated with lipopolysaccharide (LPS)-induced liver injury of HSC [28]. Interestingly, genes suppressed by LPS were re-expressed in response to erlotinib in CCl_4 mice (normalized enrichment score (NES)=-1.42, FDR=0.066), whereas no such enrichment was observed in DEN rats (NES=0.86, FDR=0.67). This further supports our data indicating that erlotinib suppresses liver injury more significantly in CCl_4 mice.

Compared to what has been reported previously in models of regeneration [23], we see a similar decrease in hepatocyte proliferation after EGFR inhibition, but we did not observe that EGFR conveyed anti-apoptotic signals to hepatocytes. Instead, we observed less liver injury suggesting that EGFR inhibition might have a role in protecting hepatocytes and this could be one mechanism by which erlotinib reduces fibrosis development. This difference will need to be examined further, but it is interesting to note that EGFR can promote both proliferation and apoptosis of HSC [27].

Further rationale for clinical evaluation of EGFR inhibition comes from studies demonstrating that EGFR is a co-factor important for hepatitis C virus (HCV) entry into cells [29]. EGF accelerates HCV entry, and EGFR tyrosine kinase inhibitors -- including erlotinib -- have substantial antiviral activity. Given the prevalence of chronic HCV infection as a source of hepatic fibrosis and cirrhosis, these observations suggest that EGFR inhibition could be a new approach to simultaneously reduce fibrotic damage previously caused by the virus and treat HCV infection.

We observed that several EGFR ligands were increased in the DEN, CCl_4 and BDL models and that treatment with erlotinib generally reduced their expression. Interestingly, EGFR ligands could have conflicting roles in liver fibrogenesis as amphiregulin (AREG) has been shown to promote liver fibrosis [30], whereas heparin-binding EGF-like growth factor (HB-EGF) suppresses liver fibrosis [31]. The relative importance of each of these ligands in liver disease will need to be elucidated in future studies especially given recent findings that EGFR ligands also play a role in HCC acquired resistance to sorafenib [32].

Another small-molecule EGFR inhibitor, gefitinib, has been previously shown to reduce the number of HCC nodules, but that effect was attributed to the anti-neoplastic effect of EGFR inhibition on the tumors themselves [13]. No investigation was reported on the effect of gefitinib on liver injury, fibrogenesis, or synthetic function. In contrast, we observed a marked impact in the surrounding non-tumoral liver tissue, but no effect of erlotinib within HCC tumors. Our analyses indicate that the effect of EGFR inhibition with erlotinib is

purely on the surrounding liver thereby reducing the risk of malignant transformation (the "field effect") rather than a direct anti-neoplastic effect on tumors. The observed reduction in small tumors after erlotinib treatment rather than an effect on the growth of existing tumors is consistent with the ability of erlotinib to suppress the initiation of HCC tumors.

Indeed, our recent studies in predicting HCC survival suggest that non-tumoral liver gene expression profiles are more predictive of clinical outcome than the profiles of the tumors themselves [6, 7]. We also note that the therapeutic benefit of EGFR inhibition in the treatment of established HCC is modest at best; only a minority of patients treated with erlotinib exhibited disease control [33, 34]. These clinical results are consistent with our observation that the most dramatic effects of EGFR blockade are on the prevention of fibrosis and cirrhosis, the principle risk factors for the development of HCC.

One potential problem with the design of anti-fibrotic and/or HCC prevention clinical trials is the lack of a sensitive way to assess treatment efficacy, as changes in liver biopsy histology might only occur after long periods and are also prone to considerable sampling error [35]. We observed that the poor-prognosis cirrhosis gene signature was completely induced in DEN-injured livers before there were any notable changes in liver function tests or liver histology, and that it was reversed in response to erlotinib. Therefore, this poor-prognosis cirrhosis signature may be useful not only for the early detection of liver fibrosis and hepatocellular transformation-associated events but also for monitoring therapeutic efficacy of chemoprevention agents.

The details of the mechanisms by which erlotinib reduces liver injury, fibrogenesis and HCC development remain to be worked out. Several different cell populations in the liver express EGFR and may each play contributory and interactive roles. It could be that erlotinib reduces the proliferation of hepatocytes, as indicated by Ki67 staining, and this directly prevents neoplastic transformation and indirectly prevents HSC activation through paracrine signaling. Consistent with this, erlotinib decreased the expression of several pro-fibrogenic factors. However, our data also demonstrates that EGFR is activated in HSC and therefore erlotinib could directly inhibit HSC activation while at the same time reducing paracrine signals that stimulate hepatocyte proliferation. We suspect that both of these mechanisms are operant, and plan to examine the relative importance of hepatocytes and HSC on the efficacy of erlotinib in follow-up studies using cellspecific targeting and genetic models. Regardless, our results in three different preclinical models of liver fibrosis suggest that EGFR is an important mediator of disease progression.

To our knowledge, this is the first demonstration that EGFR inhibition regresses liver fibrosis. The results reported here have immediate and important clinical translational implications for both hepatic fibrosis and HCC. Cirrhosis exerts an enormous toll on human health worldwide, and there is great need for interventions to slow or even regress disease progression. As for HCC, identification of high-risk populations suitable for screening and chemoprevention has been proposed as the most efficient strategy to abrogate HCC-related mortality [36]. And such high-risk populations within patients with early-stage cirrhosis may be more effectively identified with *EGF* genotype [10] and/or liver gene expression profiles [6, 7] in combination with clinical and pathologic parameters [37]. The present studies

support the evaluation of EGFR inhibitors in clinical trials of cirrhosis patients at high risk of progression and HCC development.

Supplementary Material

Refer to Web version on PubMed Central for supplementary material.

Acknowledgments

The authors would like to thank Scott Friedman and Young-Min Lee (Mount Sinai School of Medicine, New York, NY) for helpful advice on staining of HSC.

Financial Support: This work was supported by the National Institutes of Health (grant numbers K01 CA140861 to B.C.F., R01 DK099558 to Y.H. and R01 CA076183 to K.K.T.); the Massachusetts General Hospital Executive Committee on Research Fund for Medical Discovery to B.C.F.; Aid for Cancer Research to B.C.F.; the European Commission 7th Framework Programme FP7-Health 2010 (Heptromic) to Y.H.; the Howard Hughes Medical Institute to T.R.G.; and the Tucker Gosnell Center for Gastrointestinal Cancers to K.K.T.

Abbreviations

(HCC)	hepatocellular carcinoma
(EGF)	epidermal growth factor
(EGFR)	EGF receptor
(HSC)	hepatic stellate cell
(DEN)	diethylnitrosamine
(CCl_4)	carbon tetrachloride
(BDL)	bile duct ligation
(IQR)	interquartile range
(IP)	intraperitoneal
(ALP)	alkaline phosphatase
(ALT)	alanine transaminase
(AST)	aspartate transaminase
(TBIL)	total bilirubin
(Glu)	glucose
(Alb)	albumin
(CYP2E1)	cytochrome P450 2E1
(FDR)	false discovery rate
(ERK)	p44/42 mitogen-activated protein kinase
(PCNA)	proliferating cell nuclear antigen
(PDGFR-β)	platelet-derived growth factor receptor-beta
(α-SMA)	alpha-smooth muscle actin

(GFAP)	glial fibrillary acidic protein
(GSEA)	gene set enrichment analysis
(LPS)	lipopolysaccharide
(NES)	normalized enrichment score
(HCV)	hepatitis C virus
(AREG)	amphiregulin
(HB-EGF)	heparin-binding EGF-like growth factor

References

1. Jemal A, Bray F, Center MM, Ferlay J, Ward E, Forman D. Global cancer statistics. CA: A Cancer Journal for Clinicians. 2011; 61:69–90. [PubMed: 21296855]
2. El-Serag HB. Hepatocellular carcinoma. N Eng J Med. 2011; 365:1118–1127.
3. Schuppan D, Afdhal NH. Liver cirrhosis. Lancet. 2008; 371:838–851. [PubMed: 18328931]
4. Zhang DY, Friedman SL. Fibrosis-dependent mechanisms of hepatocarcinogenesis. Hepatology. 2012; 56:769–775. [PubMed: 22378017]
5. Komuves LG, Feren A, Jones AL, Fodor E. Expression of epidermal growth factor and its receptor in cirrhotic liver disease. J Histochem Cytochem. 2000; 48:821–830. [PubMed: 10820155]
6. Hoshida Y, Villanueva A, Sangiovanni A, Sole M, Hur C, Andersson KL, Chung RT, et al. Prognostic gene-expression signature for patients with hepatitis C-related early-stage cirrhosis. Gastroenterology. 2013; 144:1024–1030. [PubMed: 23333348]
7. Hoshida Y, Villanueva A, Kobayashi M, Peix J, Chiang DY, Camargo A, Gupta S, et al. Gene expression in fixed tissues and outcome in hepatocellular carcinoma. N Engl J Med. 2008; 359:1995–2004. [PubMed: 18923165]
8. Falleti E, Cmet S, Fabris C, Bitetto D, Cussigh A, Fornasiere E, Bignulin E, et al. Association between the epidermal growth factor rs4444903 G/G genotype and advanced fibrosis at a young age in chronic hepatitis C. Cytokine. 2012; 57:68–73. [PubMed: 22122913]
9. Cmet S, Fabris C, Fattovich G, Falleti E, Bitetto D, Cussigh A, Fontanini E, et al. Carriage of the EGF rs4444903 A > G functional polymorphism associates with disease progression in chronic HBV infection. Clin Exp Immunol. 2012; 167:296–302. [PubMed: 22236006]
10. Tanabe KK, Lemoine A, Finkelstein DM, Kawasaki H, Fujii T, Chung RT, Lauwers GY, et al. Epidermal growth factor gene functional polymorphism and the risk of hepatocellular carcinoma in patients with cirrhosis. JAMA. 2008; 299:53–60. [PubMed: 18167406]
11. Tonjes RR, Lohler J, O'Sullivan JF, Kay GF, Schmidt GH, Dalemans W, Pavirani A, et al. Autocrine mitogen IgEGF cooperates with c-myc or with the Hcs locus during hepatocarcinogenesis in transgenic mice. Oncogene. 1995; 10:765–768. [PubMed: 7862454]
12. Lee TY, Kim KT, Han SY. Expression of ErbB receptor proteins and TGF-alpha during diethylnitrosamine-induced hepatocarcinogenesis in the rat liver. Korean J Hepatol. 2007; 13:70–80. [PubMed: 17380077]
13. Schiffer E, Housset C, Cacheux W, Wendum D, Desbois-Mouthon C, Rey C, Clergue F, et al. Gefitinib, an EGFR inhibitor, prevents hepatocellular carcinoma development in the rat liver with cirrhosis. Hepatology. 2005; 41:307–314. [PubMed: 15660382]
14. Ishak KG. Chronic hepatitis: morphology and nomenclature. Mod Pathol. 1994; 7:690–713. [PubMed: 7991529]
15. Fujii T, Fuchs BC, Yamada S, Lauwers GY, Kulu Y, Goodwin JM, Lanuti M, et al. Mouse model of carbon tetrachloride induced liver fibrosis: Histopathological changes and expression of CD133 and epidermal growth factor. BMC Gastroenterol. 2010; 10:79. [PubMed: 20618941]

16. Hoshida Y, Fuchs BC, Tanabe KK. Prevention of hepatocellular carcinoma: potential targets, experimental models, and clinical challenges. Curr Cancer Drug Targets. 2012; 12:1129–1159. [PubMed: 22873223]

17. Kang JS, Wanibuchi H, Morimura K, Gonzalez FJ, Fukushima S. Role of CYP2E1 in diethylnitrosamine-induced hepatocarcinogenesis in vivo. Cancer Res. 2007; 67:11141–11146. [PubMed: 18056438]

18. Wong FW, Chan WY, Lee SS. Resistance to carbon tetrachloride-induced hepatotoxicity in mice which lack CYP2E1 expression. Toxicol Appl Pharmacol. 1998; 153:109–118. [PubMed: 9875305]

19. Seok J, Warren HS, Cuenca AG, Mindrinos MN, Baker HV, Xu W, Richards DR, et al. Genomic responses in mouse models poorly mimic human inflammatory diseases. Proc Narl Acad Sci USA. 2013; 110:3507–3512.

20. Kuriyama S, Yokoyama F, Inoue H, Takano J, Ogawa M, Kita Y, Yoshiji H, et al. Sequential assessment of the intrahepatic expression of epidermal growth factor and transforming growth factor-beta1 in hepatofibrogenesis of a rat cirrhosis model. Int J Mol Med. 2007; 19:317–324. [PubMed: 17203207]

21. Sorkin A, Goh LK. Endocytosis and intracellular trafficking of ErbBs. Exp Cell Res. 2009; 315:683–696. [PubMed: 19278030]

22. Berasain C, Perugorria MJ, Latasa MU, Castillo J, Goni S, Santamaria M, Prieto J, et al. The epidermal growth factor receptor: a link between inflammation and liver cancer. Exp Biol Med. 2009; 234:713–725.

23. Natarajan A, Wagner B, Sibilia M. The EGF receptor is required for efficient liver regeneration. Proc Natl Acad Sci USA. 2007; 104:17081–17086. [PubMed: 17940036]

24. Friedman SL. Mechanisms of hepatic fibrogenesis. Gastroenterology. 2008; 134:1655–1669. [PubMed: 18471545]

25. Friedman SL. Hepatic stellate cells: protean, multifunctional, and enigmatic cells of the liver. Physiol Rev. 2008; 88:125–172. [PubMed: 18195085]

26. Yang C, Zeisberg M, Mosterman B, Sudhakar A, Yerramalla U, Holthaus K, Xu L, et al. Liver fibrosis: insights into migration of hepatic stellate cells in response to extracellular matrix and growth factors. Gastroenterology. 2003; 124:147–159. [PubMed: 12512039]

27. Sommerfeld A, Reinehr R, Haussinger D. Bile acid-induced epidermal growth factor receptor activation in quiescent rat hepatic stellate cells can trigger both proliferation and apoptosis. J Biol Chem. 2009; 284:22173–22183. [PubMed: 19553664]

28. Seki E, De Minicis S, Osterreicher CH, Kluwe J, Osawa Y, Brenner DA, Schwabe RF. TLR4 enhances TGF-beta signaling and hepatic fibrosis. Nat Med. 2007; 13:1324–1332. [PubMed: 17952090]

29. Lupberger J, Zeisel MB, Xiao F, Thumann C, Fofana I, Zona L, Davis C, et al. EGFR and EphA2 are host factors for hepatitis C virus entry and possible targets for antiviral therapy. Nat Med. 2011; 17:589–595. [PubMed: 21516087]

30. Perugorria MJ, Latasa MU, Nicou A, Cartagena-Lirola H, Castillo J, Goni S, Vespasiani-Gentilucci U, et al. The epidermal growth factor receptor ligand amphiregulin participates in the development of mouse liver fibrosis. Hepatology. 2008; 48:1251–1261. [PubMed: 18634036]

31. Huang G, Besner GE, Brigstock DR. Heparin-binding epidermal growth factor-like growth factor suppresses experimental liver fibrosis in mice. Lab Invest. 2012; 92:703–712. [PubMed: 22330337]

32. Blivet-Van Eggelpoel MJ, Chettouh H, Fartoux L, Aoudjehane L, Barbu V, Rey C, Priam S, et al. Epidermal growth factor receptor and HER-3 restrict cell response to sorafenib in hepatocellular carcinoma cells. J Hepatol. 2012; 57:108–115. [PubMed: 22414764]

33. Philip PA, Mahoney MR, Allmer C, Thomas J, Pitot HC, Kim G, Donehower RC, et al. Phase II study of Erlotinib (OSI-774) in patients with advanced hepatocellular cancer. J Clin Oncol. 2005; 23:6657–6663. [PubMed: 16170173]

34. Thomas MB, Chadha R, Glover K, Wang X, Morris J, Brown T, Rashid A, et al. Phase 2 study of erlotinib in patients with unresectable hepatocellular carcinoma. Cancer. 2007; 110:1059–1067. [PubMed: 17623837]

35. Popov Y, Schuppan D. Targeting liver fibrosis: strategies for development and validation of antifibrotic therapies. Hepatology. 2009; 50:1294–1306. [PubMed: 19711424]

36. Llovet JM, Burroughs A, Bruix J. Hepatocellular carcinoma. Lancet. 2003; 362:1907–1917. [PubMed: 14667750]

37. Lok AS, Seeff LB, Morgan TR, di Bisceglie AM, Sterling RK, Curto TM, Everson GT, et al. Incidence of hepatocellular carcinoma and associated risk factors in hepatitis C-related advanced liver disease. Gastroenterology. 2009; 136:138–148. [PubMed: 18848939]

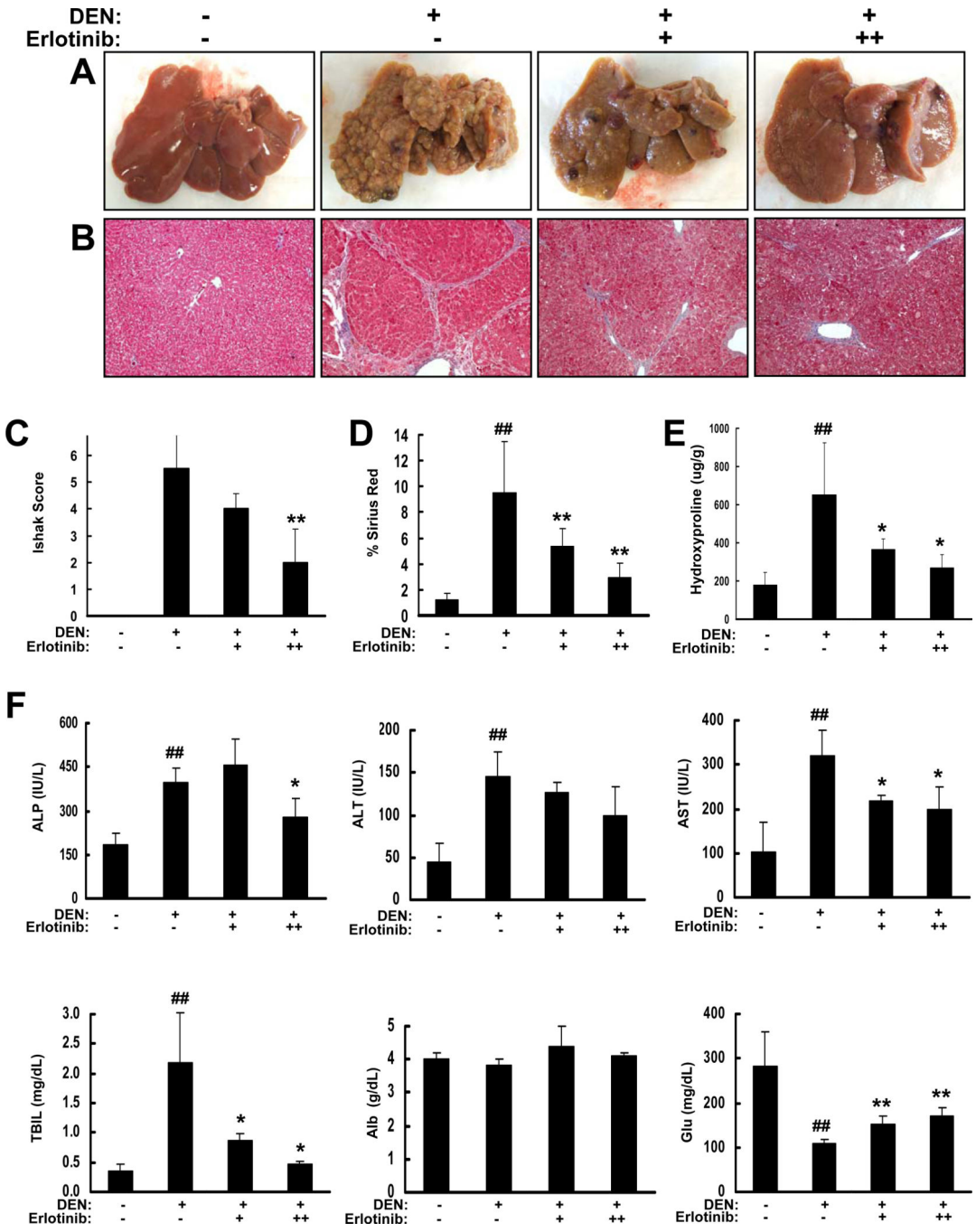

Figure 1. Erlotinib inhibits DEN-induced cirrhosis in rats

Male Wistar rats received PBS (−) or DEN (+) for 18 weeks. DEN-injured rats received vehicle control (−) or erlotinib (0.5 (+) or 2 mg/kg (++)) during weeks 13 – 18. **(A)** Representative rat livers at the time of sacrifice. **(B)** Representative trichrome staining of FFPE liver tissue (Magnification 100X). **(C)** Trichrome stains were scored by the method of Ishak. Collagen levels were **(D)** morphometrically quantified from Sirius red stained sections or **(E)** assessed by hydroxproline analysis. **(F)** Serum levels (N = 4 for all groups) of alkaline phosphatase (ALP), alanine transaminase (ALT), aspartate transaminase (AST),

total bilirubin (TBIL), albumin (Alb) and glucose (Glu). ## $p < 0.01$ compared to PBS, * $p < 0.05$ and ** $p < 0.01$ compared to DEN-injured.

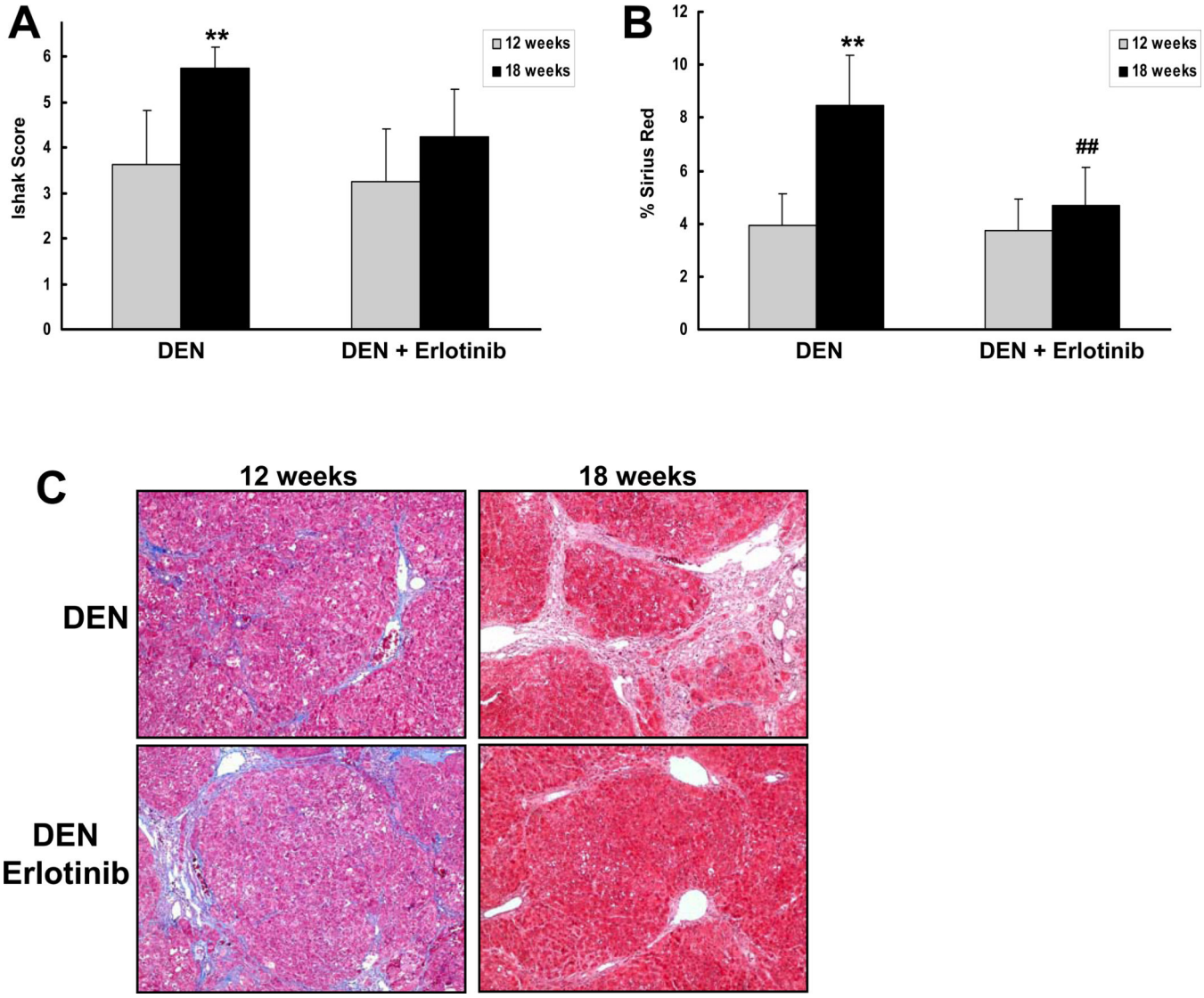

Figure 2. Erlotinib regresses cirrhosis progression in a subset of DEN-injured rats

Male Wistar rats received DEN for 18 weeks. After 12 weeks, the rats underwent a survival hepatectomy and a liver biopsy was removed for histology. Rats then received 2 mg/kg erlotinib or vehicle during weeks 13 – 18. **(A)** Trichrome stains from each animal before and after treatment with vehicle or erlotinib were scored by the method of Ishak. **(B)** Collagen levels were morphometrically quantified from Sirius red stained sections. **(C)** Representative trichome stains of a vehicle control animal whose disease progressed and an erlotinib animal whose disease regressed. **$p < 0.01$ compared to DEN-injured 12 weeks and ## $p < 0.01$ compared to DEN-injured, erlotinib-treated 12 weeks.

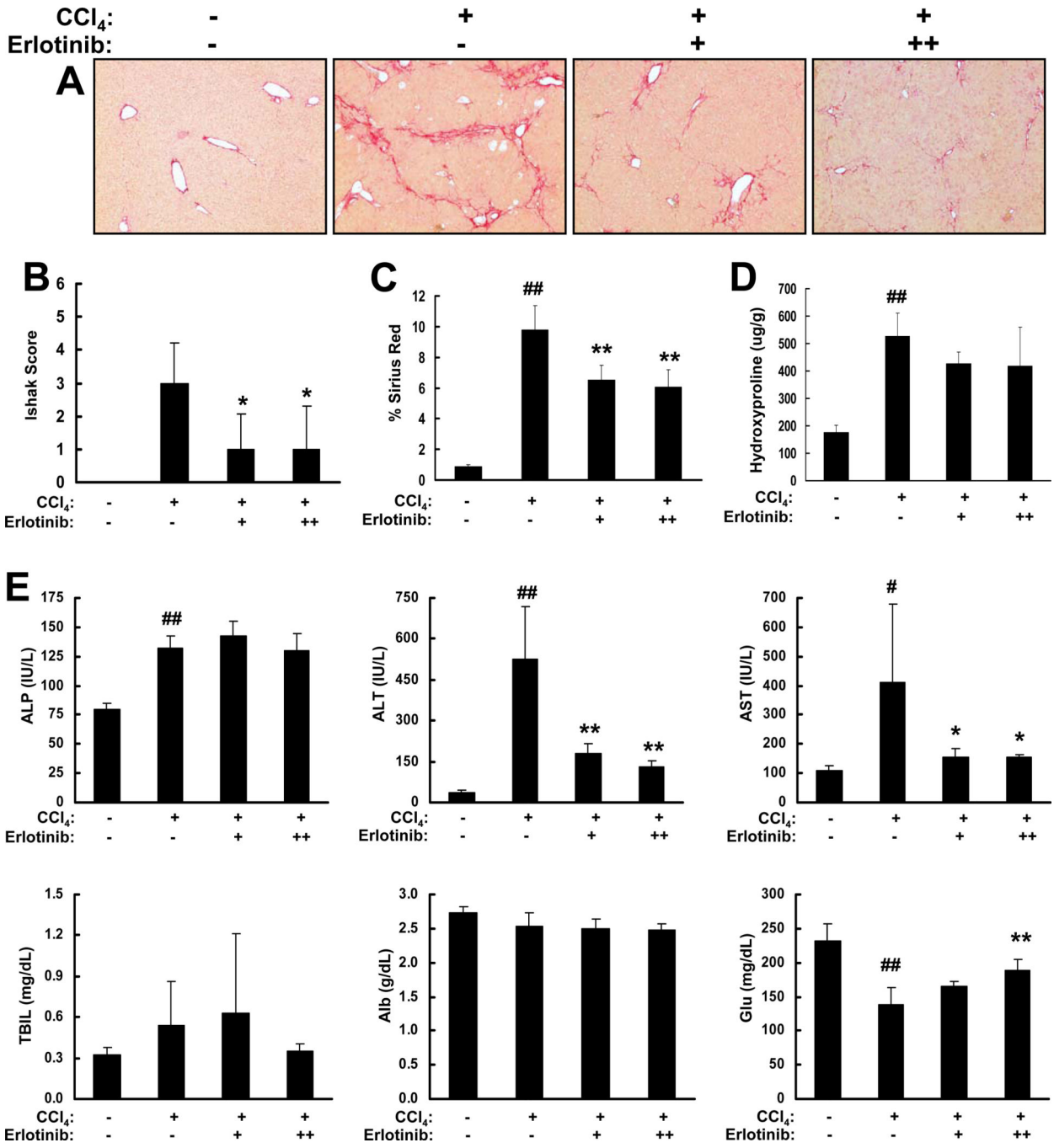

Figure 3. Erlotinib inhibits CCl_4-induced fibrosis in mice

Male A/J mice were administered either 0.1cc of a 40% solution of CCl_4 in olive oil (+) or olive oil alone (−) for 18 weeks. CCl_4-injured mice received IP injections of vehicle control (−) or erlotinib (2 (+) or 5 mg/kg (++)) during weeks 13 – 18. **(A)** Representative Sirius red staining of FFPE mouse liver tissue (Magnification 100X). **(B)** Trichrome stains of liver sections from each animal were scored by the method of Ishak. Collagen levels were **(C)** morphometrically quantified from Sirius red stained sections or **(D)** assessed by hydroxproline analysis. **(E)** Serum levels (N = 4 for all groups) of alkaline phosphatase

(ALP), alanine transaminase, aspartate transaminase, total bilirubin (TBIL), albumin (Alb) and glucose (Glu). # $p < 0.05$ and ## $p < 0.01$ compared to olive oil, * $p < 0.05$ and ** $p < 0.01$ compared to CCl_4-injured.

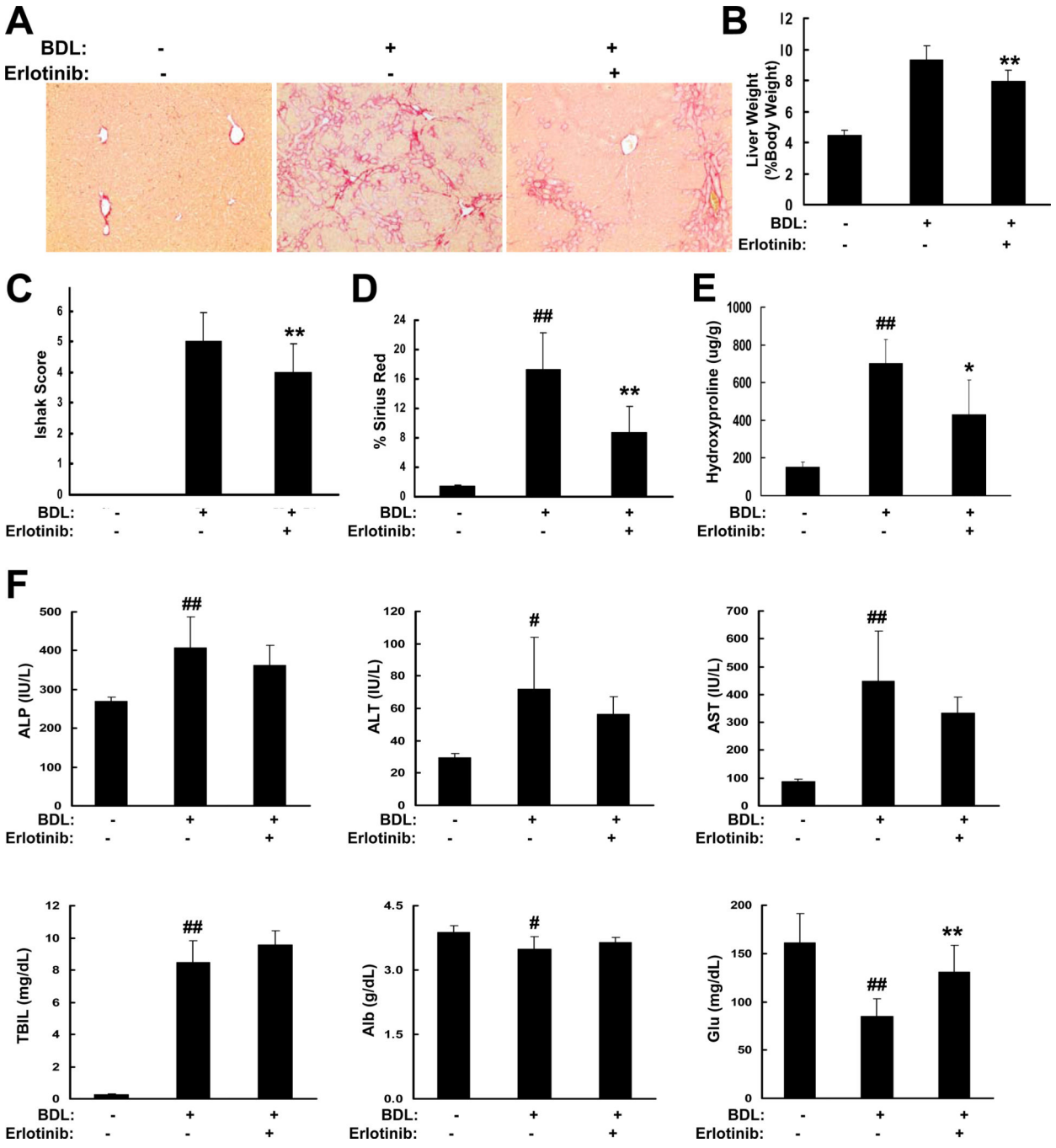

Figure 4. Erlotinib inhibits biliary fibrosis in BDL rats

Male Wistar rats that had undergone a sham operation (−) or BDL (+) received IP injections of vehicle control (−) or erlotinib (2 mg/kg (+)) beginning 4 days after the BDL and ending on Day 21. **(A)** Representative Sirius red staining of FFPE rat liver tissue (Magnification 100X). **(B)** Liver weight is expressed as percent body weight. **(C)** Trichrome stains of liver sections from each animal were scored by the method of Ishak. Collagen levels were **(D)** morphometrically quantified from Sirius red stained sections or **(E)** assessed by hydroxproline analysis. **(F)** Serum levels (N = 5 for all groups) of alkaline phosphatase

(ALP), alanine transaminase, aspartate transaminase, total bilirubin (TBIL), albumin (Alb) and glucose (Glu). # $p < 0.05$ and ## $p < 0.01$ compared to sham operation, * $p < 0.05$ and ** $p < 0.01$ compared to BDL.

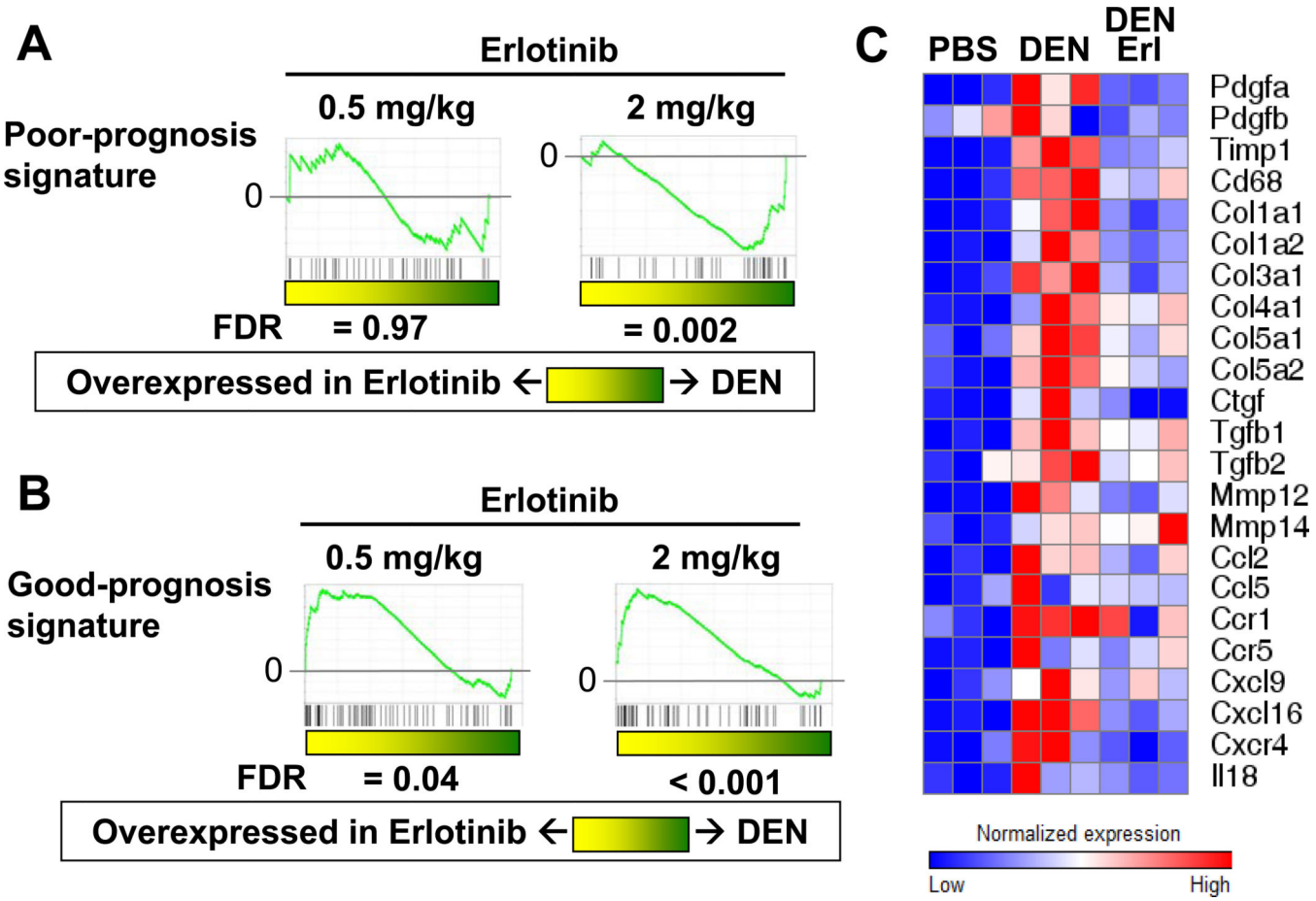

Figure 5. Erlotinib reverses a gene expression signature associated with poor survival in human cirrhosis and HCC patients

Male Wistar rats received PBS or DEN for 8, 12 or 18 weeks. DEN-injured rats received erlotinib (0.5 or 2 mg/kg) during weeks 13 – 18. GSEA analysis of the **(A)** 73-gene poor-prognosis signature and **(B)** 113- gene good-prognosis signature in DEN rats after treatment with erlotinib. **(C)** Heat maps are shown for several pro-fibrogenic genes.

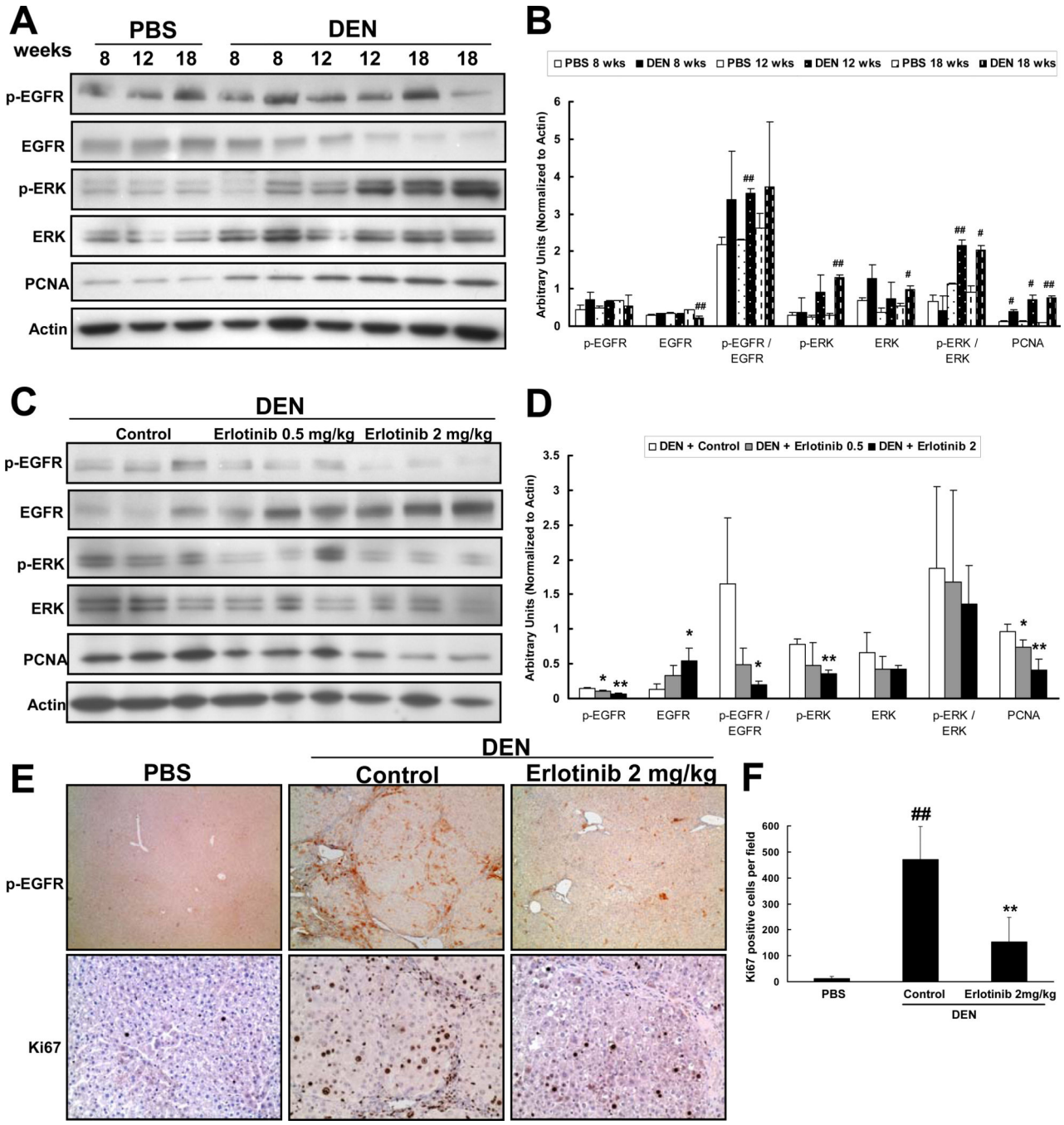

Figure 6. Erlotinib decreases EGFR signaling

(A) Representative western blot analysis performed on non-tumoral surrounding liver tissue lysates from every PBS and DEN animal and **(B)** quantification of these blots. # $p < 0.05$ or ## $p < 0.01$ compared to PBS **(C)** Representative western blot analysis performed on every DEN-injured animal after treatment with vehicle (Control) or Erlotinib 0.5 mg/kg or Erlotinib 2 mg/kg and **(D)** quantification of these blots. * $p < 0.05$ or ** $p < 0.01$ compared to DEN-injured. **(E)** Representative photomicrographs of liver sections from PBS and DEN-injured animals after treatment with vehicle (Control) or Erlotinib 2 mg/kg that were stained

for phospho- EGFR (Magnification 40X) or Ki67 (Magnification 200X). **(F)** Ki67 stainings were quantified. ## $p < 0.01$ compared to PBS, ** $p < 0.01$ compared to DEN-injured.

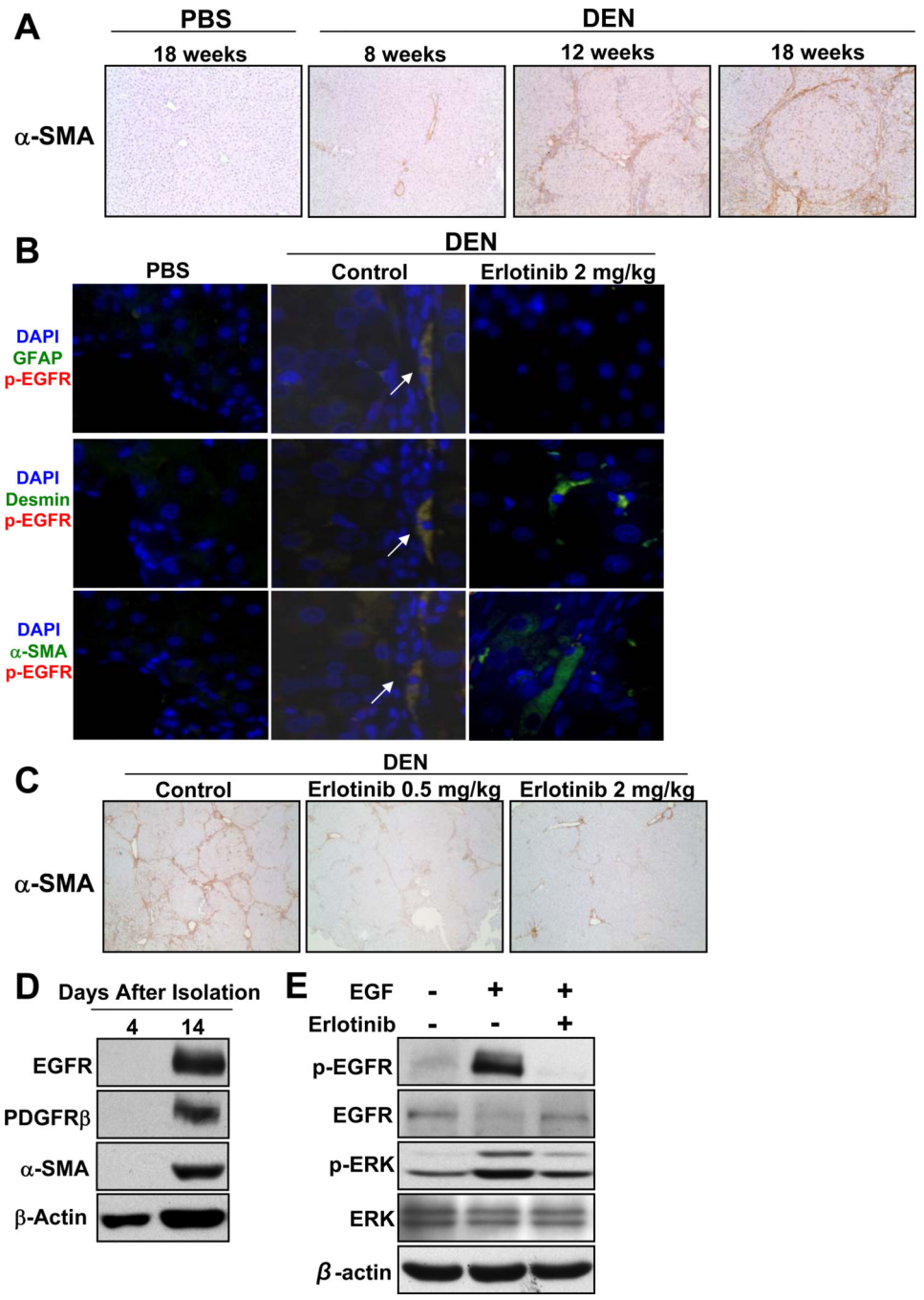

Figure 7. DEN administration activates HSC through increased EGFR signaling which is inhibited by erlotinib

Male Wistar rats received PBS or DEN for 18 weeks. DEN-injured rats received erlotinib (0.5 or 2 mg/kg) during weeks 13 – 18. **(A)** Representative photomicrographs of liver sections from PBS or DEN rats that were stained for α-SMA (Magnification 100X). **(B)** Liver sections from rats that received PBS as well as DEN-injured rats treated with vehicle (Control) or Erlotinib 2 mg/kg were costained for p-EGFR (Y1068) and either GFAP, desmin or α-SMA (Magnification 400X). **(C)** Representative photomicrographs of liver

sections from DEN rats treated with erlotinib that were stained for α-SMA (Magnification 40X). Representative western blot analysis of **(D)** primary rat HSCs grown in culture for either 4 or 14 days and **(E)** primary rat HSCs treated with 100 ng/ml EGF in the absence of presence of 2 μM erlotinib for 30 minutes.

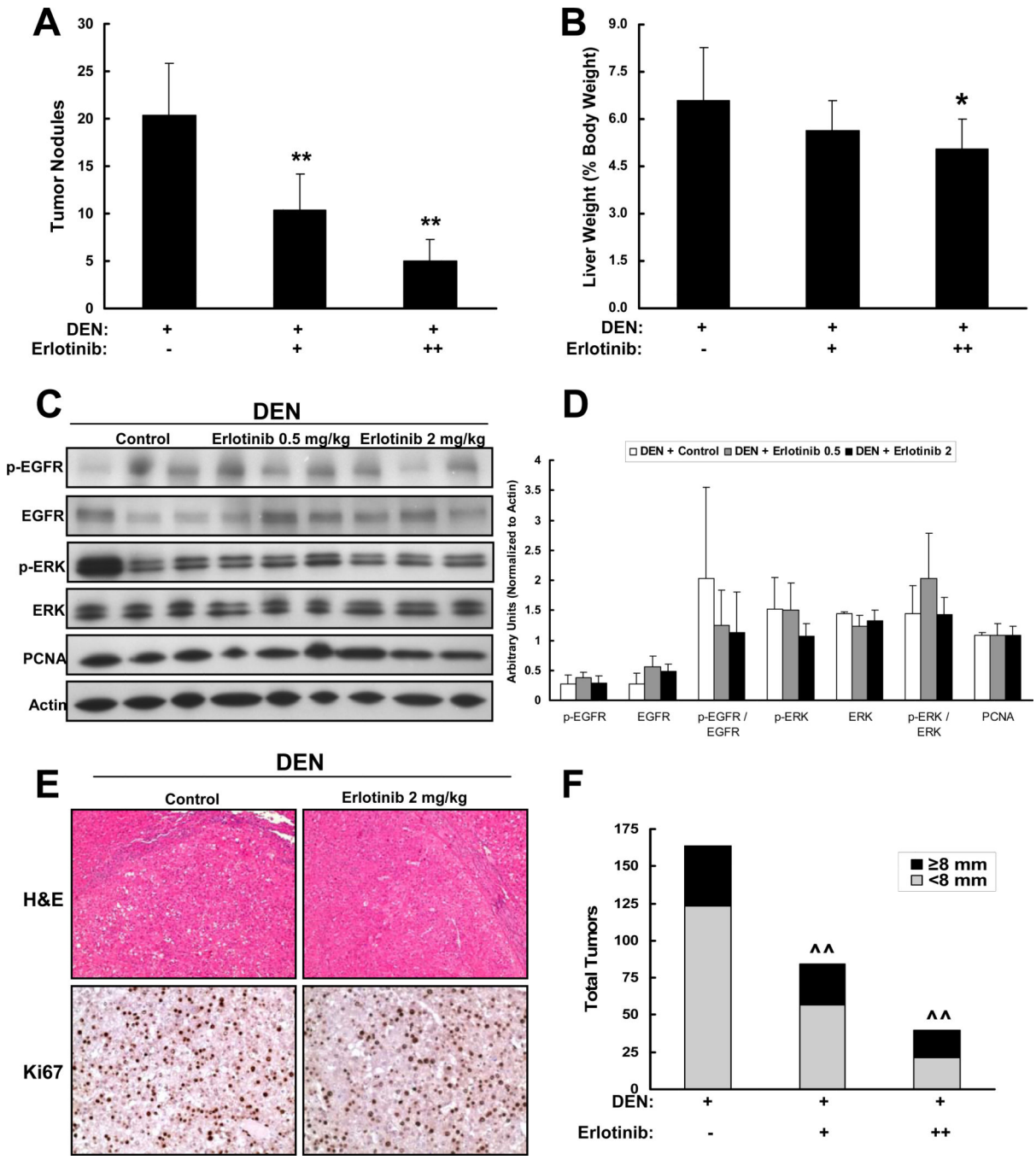

Figure 8. Erlotinib decreases HCC development by inhibiting cirrhosis progression

Male Wistar rats received DEN (+) for 18 weeks. Rats received vehicle control (−) or erlotinib (0.5 (+) or 2 mg/kg (++)) during weeks 13 – 18. **(A)** Tumors that were greater than 5 mm in diameter were counted. **(B)** Liver weight is expressed as percent body weight. **(C)** Representative western blot analysis on liver tumor lysates from every animal in each group and **(D)** quantification of these blots. **(E)** Representative photomicrographs of tumor sections from DEN-injured rats treated with vehicle (Control) or erlotinib 2 mg/kg that were stained for H-E (Magnification 100X) or Ki67 (Magnification 200X). **(F)** Tumors from

every animal were measured at the time of sacrifice. The proportion of smaller tumors (those that measured < 8 mm (i.e. < the 75^{th} percentile)) was decreased by erlotinib in a dose-dependent manner. * $p < 0.05$ and ** $p < 0.01$ compared to DEN-injured. ^^ $p = 0.01$ Fisher's exact test and $p = 0.003$ Cochran-Armitage test for trend of proportion.